

AEROSOL EFFECTS ON MESOSCALE STRUCTURES IN MARINE BOUNDARY LAYER CLOUDS

FDL Europe 2020: Clouds & Aerosols, Technical Memorandum

Matt Christensen, University of Oxford

Will Jones, University of Oxford

Matt Kusner, University College London

Lucas Kruitwagen, University of Oxford

Tim Pearce, University of Cambridge

Sorawit Saengkyongam, University of Copenhagen

Duncan Watson-Parris, University of Oxford



Tim Pearce
ML Researcher



Sorawit Saengkyongam
ML Researcher



Will Jones
Clouds Researcher



Lucas Kruitwagen
Climate Researcher



Matt Kusner
ML Lead



Matt Christensen
Domain Lead



Duncan Watson-Parris
Super Mentor

August 2020

Acknowledgments: This work has been enabled by Frontier Development Lab (FDL) Europe (<https://fdleurope.org>) a public / private partnership between the European Space Agency (ESA), Trillium Technologies and the University of Oxford (<http://www.ox.ac.uk>), and supported by Google Cloud, NVidia, and Scan UK.

AEROSOL EFFECTS ON MESOSCALE STRUCTURES IN MARINE BOUNDARY LAYER CLOUDS

Matt Christensen, University of Oxford

Will Jones, University of Oxford

Matt Kusner, University College London

Lucas Kruitwagen, University of Oxford

Tim Pearce, University of Cambridge

Sorawit Saengkyongam, University of Copenhagen

Duncan Watson-Parris, University of Oxford

Frontier Development Lab Europe 2020: Clouds & Aerosols Technical Memorandum

ABSTRACT

Acknowledgments: This work has been enabled by Frontier Development Lab (FDL) Europe (<https://fdleurope.org>) a public / private partnership between the European Space Agency (ESA), Trillium Technologies and the University of Oxford (<http://www.ox.ac.uk>), and supported by Google Cloud, NVidia, and Scan UK. This work also benefited from the support of non-author contributors. Ricardo Silva and Sebastian Weichwald advised us on causal methods. Rob Wood, Philip Stier and Ed Gryspeerdt advised us on cloud and aerosol interactions. We are immensely grateful for their time and insight, without which our success would have been impossible.

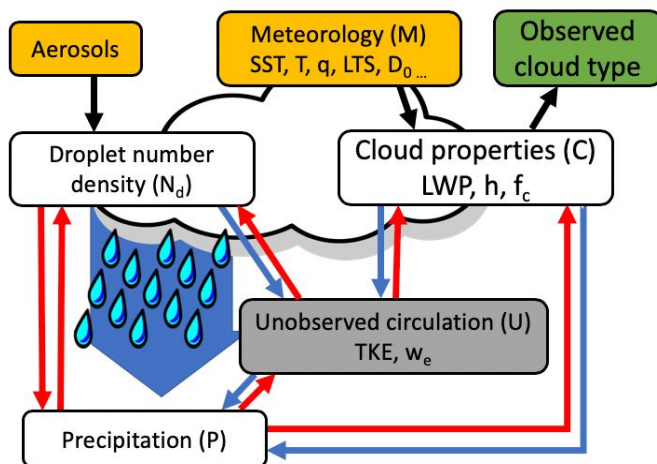
INTRODUCTION

Marine boundary layer (MBL) clouds cover a vast area of the world's oceans. In doing so, they reflect a large portion of incoming solar radiation, and so have a significant cooling impact on the planetary energy budget. In particular, the large stratocumulus cloud decks off of the Western seaboard of North and South America, Australia, and Africa have a strong cooling effect due to their great extent (measuring thousands of kms across) and proximity to the equator. Even a small change in the properties of these cloud decks could have significant impacts on future climate change.

Clouds are affected by human activity through their feedbacks to climate change, but also directly due to aerosol-cloud interactions (ACI). Aerosols (particulate pollutants suspended in the atmosphere) interact with clouds by forming condensation nuclei which cloud droplets form around. An increase in aerosols leads to an increase in cloud droplets, and hence an increase of the reflectivity of the cloud. This causes a cooling effect, which historically has offset a significant portion of global warming due to greenhouse gases. These changes to cloud droplets may also influence the size and lifetime of clouds through their impacts on precipitation and evaporation processes. These secondary ACI are highly uncertain, but may have significant impacts on the climate.

MBL clouds exhibit a range of meso-scale structures which not only have different radiative impacts upon the climate. Furthermore, ACI effects affect, and are affected by, these meso-scale structures. The relationship between ACI effects and meso-scale structures is governed by a range of physical processes, some of which are unobservable, see Figure 1.

Figure 1: ACI processes



Using observations from EUMETSAT's MSG SEVIRI imager over the Southern Atlantic Ocean, we aim to better understand the aerosol impact on cloud structure through the application of multiple machine learning methods. We use unsupervised and self-supervised learning to observe cloud meso-scale structures - 'cloud types'. We then use a recurrent neural network to isolate the causal impacts of aerosols on our observed cloud types.

Our findings relating cloud types (and their radiative impacts) to aerosol concentrations have potential to reduce uncertainty in long-term climate modelling, help regional climate downscaling, and can inform debates around the risks and impacts of geoengineering proposals.

RESEARCH NEED

Cloud formation and cloud properties play a crucial role in moderating the energy balance of the Earth. Clouds play a dominant role in the Earth's albedo (i.e. the amount of energy being reflected back into space), being responsible for as much as half of these net-cooling effects.^[1] Principle among cloud formations are marine boundary layer clouds: low-altitude stratocumulus clouds covering on average 30% of the planet's oceans.^[2] Meso-scale structures in these clouds have a significant impact on the cloud formation's albedo: so-called "closed-cell" regimes have a much higher albedo than "open-cell" regimes, see Figure 2.^[3,4]

A number of physical processes have been identified which govern the formation and development of meso-scale structures, see Wood, R. (2012)^[5] for a summary. Such processes include precipitation of liquid water, entrainment (i.e. capture) of dry air, longwave cooling and solar heating of the cloud top, and fluxes of energy and water from the ocean surface. The precise relationship between these processes and other exogenous factors such as wind speed, air temperature, and sea surface temperature remains a major source of uncertainty in large-scale climate projections.

Cloud-aerosol interactions are salient physical processes impacting the formation of and transition between meso-scale cloud structures. Aerosols are fine solid particles suspended in air which can be either natural (e.g. ocean spray, dust, pollen) or anthropogenic (e.g. conventional air pollutants, smoke). Aerosols provide nuclei for condensation in clouds, increasing cloud droplet number, and decreasing droplet size, with consequences for precipitation, cloud radiative forcing, and cloud structure.^[6,7] Aerosols have also been shown to delay the transition between "closed-cell" and "open-cell" cloud regimes, with further impacts on cloud average cloud albedo.^[8] Proponents of stratospheric aerosol injection seek to use this mechanism as a form of radiative forcing geoengineering.^[9,10] Aerosol-cloud interactions are one of the largest sources of uncertainty in long-term climate modelling.^[11]

To identify the impact of aerosols on meso-scale cloud structures, first a typology of these structures must be developed. Prior work has focussed on identifying observable "cloud types" as a proxy for cloud structures, by using expert hand-labelling,^[12] supervised machine learning,^[13] and unsupervised machine learning.^[14] Hand-labelling and supervised methods encode human bias into their classification. All three of these methods rely on satellite-retrieved reflectances for a single point in time, potentially missing phenomena occurring with a less-than-immediate time latency. These studies only use visible spectra which are unavailable at night, making them unsuitable for detecting diurnal trends and processes.

With a typology of cloud types established, we can proceed to examining the causal influence of aerosols on cloud types. Several important variables in cloud processes are unobservable: the entrainment rate and turbulent kinetic energy (We and TKE respectively in Figure 1), for example. A causal analysis of the impact of aerosols on cloud properties must control for both observable and unobserved confounding properties. Fortunately a back-door adjustment^[15] is

available in the cloud property causal graph which allows these confounding factors to be marginalised.

DATA DESCRIPTION

We obtain orthorectified satellite data from several sources. Our aim is to observe meso-scale cloud structures and then study the causal processes in their formation, controlling for meteorology and other climatic processes. This necessitates a large dataframe fusing a number of data sources. We observe meso-scale cloud structures in raw SEVIRI Meteosat data obtained from EUMETSAT^[16]. We also obtain derived retrieval data based on the raw SEVIRI data from the NASA MODIS cloud product algorithms^[17]. We match our satellite data with meteorology data obtained from ECMWF’s ERA5 dataset. Finally, we add precipitation data from NASA’s IMERG^[19], and recalibrate it using a look-up-table with CloudSat^[20] rain rates to better capture low volume drizzle, which is poorly measured by IMERG. See Table 1 for a summary for data variables.

Table 1: Clouds & Aerosols Data

Dataset	Description	Source Satellite	Dataset	Description	Source Satellite
ND	Droplet Number	SEVIRI	CER	Droplet Effective Radius	SEVIRI + [17]
SOLZ	Solar Zenith Angle	SEVIRI	COT	Cloud Optical Thickness	SEVIRI + [17]
CH1	VIS0.6	SEVIRI	PR	Precipitation	IMERG
CH3	NIR1.6	SEVIRI	SST	Sea Surface Temperature	ERA5
CH4	NIR3.9	SEVIRI	LTS	Land Surface Temperature	ERA5
CH9	IR10.8	SEVIRI	FTH	Free Tropospheric Humidity	ERA5
CH10	IR12.0	SEVIRI	WS	Wind Speed	ERA5
CTT	Cloud Top Temperature	SEVIRI + [17]	DIV	Divergence	ERA5
CTH	Cloud Top Height	SEVIRI + [17]	PR_LUT	Precipitation	CloudSat
LWP	Liquid Water Path	SEVIRI + [17]			

All data is sampled at 30 minutes cadence and a 3km resolution. The area of our study is the South Atlantic cloud deck of the West coast of Africa, extending from -20.16 to 20.14 longitude and -27.08 to 3.07 latitude. The data are obtained for 66 days extending from 2017-07-07 to 2017-10-31. Several dates are missing due to incomplete retrieval data. The data were obtained from the JASMIN super-data-cluster at Science and Technology Facilities Council Rutherford Appleton Laboratory in Harwell, Oxford¹ and mirrored to Google Cloud Storage.

METHODOLOGY

We develop a methodology to study the causal impact that aerosols have on cloud meso-scale structures. We begin by developing learning methods to discover a typology of cloud structures. We also develop a novel moving reference frame - the “Lagrangian” reference frame - as a pre-processing method. Finally we develop a method for removing the observed and unobserved confounders to isolate the causal influence of aerosols on cloud type.

Unsupervised Classification

¹ For more information regarding JASMIN, see <https://www.jasmin.ac.uk/what-is-jasmin/>

We begin by adapting unsupervised classification methods to obtain cloud types. We prepare two unsupervised methods. The first reproduces Denby (2020)^[14], which is the state-of-the-art. Denby (2020)^[14] uses the tile-to-vec algorithm^[21] to obtain a latent representation of 64^2 pixel patches sampled randomly from the data. The latent representations are hierarchically clustered to obtain a cloud meso-structure typology. Tile-to-vec uses anchor-neighbour-distant triplet loss to train the embedder, where proximity is measured spatially.

The second method develops an Information Maximising Generative Adversarial Network (InfoGAN)^[22], following Yuan (2019)^[23]. An InfoGAN provides a number of controls over the features that the generator learns, allowing the researcher to disentangle the properties the generator learns. The auxiliary discriminator ('Q head') can then also be used as a classifier with the dimensions of the control space as the learned classes. See Figure 2 and 3 for schematics of the unsupervised architectures.

Figure 2: Tile-to-Vec Architecture

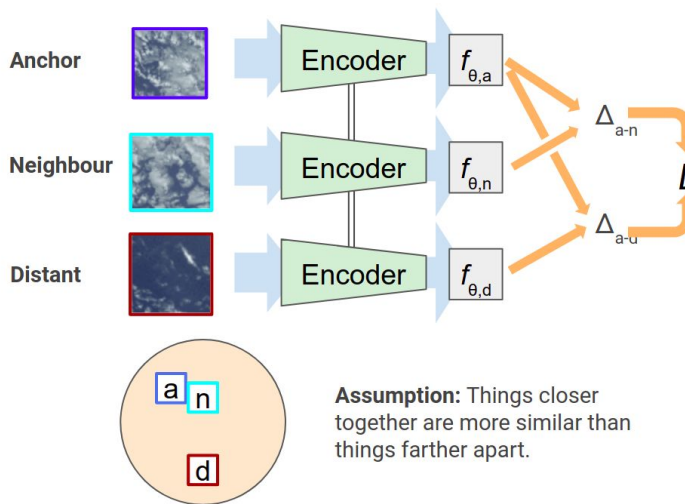
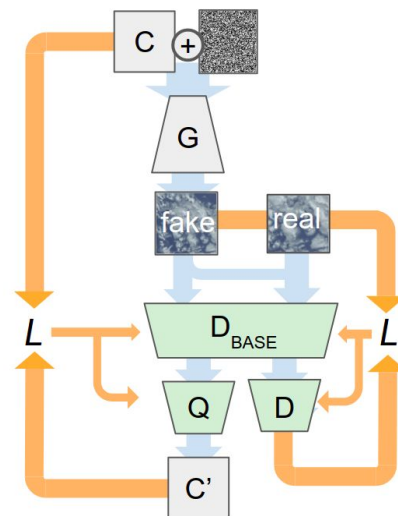


Figure 3: InfoGAN Architecture



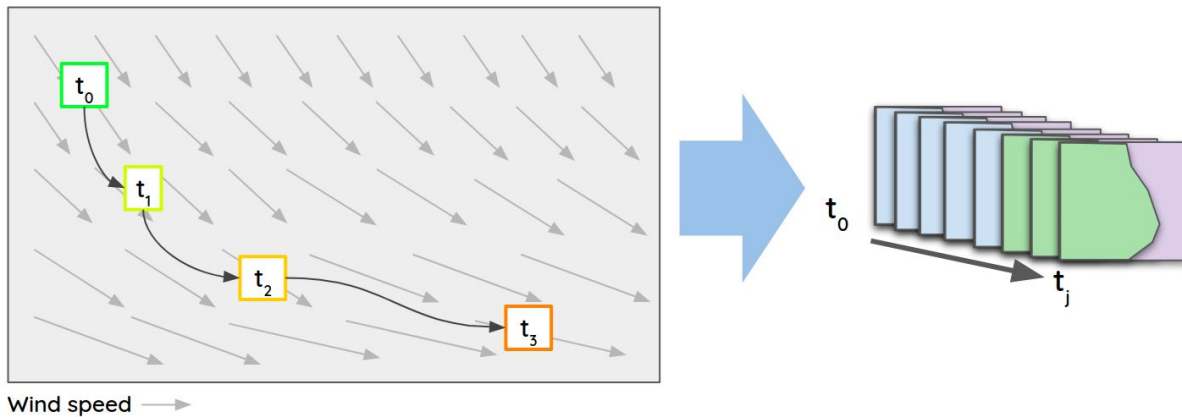
Both unsupervised classification methods produce only a single class label for the image patch. To develop a segmentation map, the convolved across the region of interest in the Southern Atlantic with an 8 pixel stride, and smoothed with a gaussian kernel.

Lagrangian Reference Frame

Following the intuition of Christiansen et al. (2020)^[24], we adopt the Lagrangian Reference Frame for our analysis. The Lagrangian reference frame follows a moving volume of air, see Figure 4 for an illustration. This moving reference frame simplifies the challenge of next-timestep prediction by ensuring that the same volume of air remains under the same pixel. We use the HYSPLIT Trajectory Model from the NOAA Air Resources Lab^[25] to track air volumes through our study area of interest and timespan. We randomly seed over 1000 starting locations per hourly time slice of our dataset and obtain 72 hour forward trajectories for each location. We clip

these trajectories to the geographic area of our study. The total dataset is comprised of over 4.5mn trajectories.

Figure 4: Lagrangian reference frame trajectories

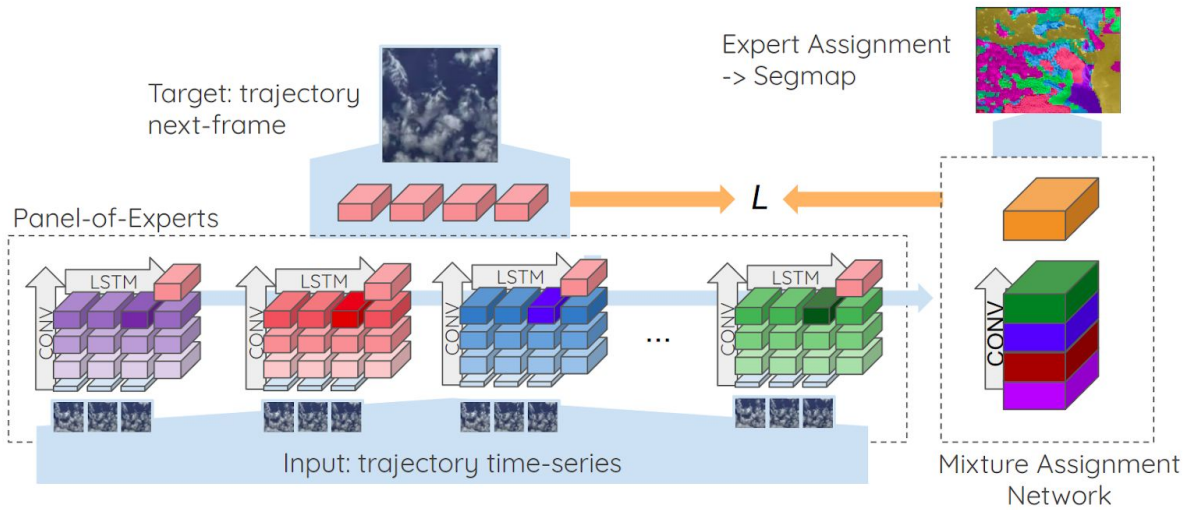


Mixture of Experts Classification

Our third approach for identifying cloud meso-scale structures adopts a classical machine learning method: the mixture of experts. We adapt an approach from Zhang, Dejiao, et al. (2017)^[26]. The intuition is that each expert should specialise in identifying a different type of cloud structure. To train our experts, we take advantage of the temporal nature of our data. We train our experts to predict the next time-step in our data, a self-supervised method. With this temporal method, we also seek to better capture processes which might be temporally lagged. Transitions between cloud types may show some hysteresis, and so using input data with multiple timesteps to predict the subsequent time step will capture temporally distributed phenomena.

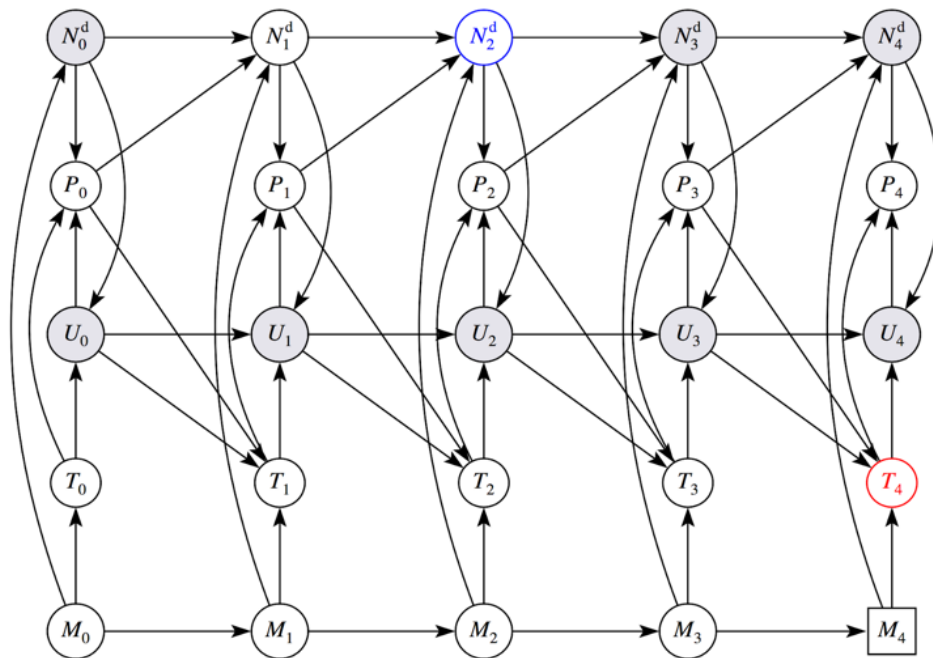
We use a Conv-LSTM encoding architecture for the self-supervised prediction task, see Figure 5. Each expert is instantiated and attempts to predict the next timestep in the lagrangian reference frame. The input data shape is thus four dimensional: time, channels, and two dimensions in the pixel space. The penultimate latent representations from each expert are concatenated into a separate ‘mixture assignment network’. The output of the mixture assignment network has three dimensions: the number of experts and the pixel space. The maximum pixel-wise activation is then used to determine which expert should be used to predict each pixel. Only losses for each pixel-wise expert are retained during training, and in this way the experts are incentivised to specialise in a specific cloud type. The mixture assignment network also then produces a classification map which can be used as a semantic segmentation.

Figure 5: Mixture-of-experts model



Causal Algorithm

Figure 6: Causal structure of the aerosol–cloud interactions



Theorem 1. The causal effect of $N_{t'}^d$ on T_t given M_t is identifiable for all $t > t'$ from observational data as follows,

$$P(T_t | do(N_{t'}^d), M_t) = \sum_{M_{t'}, N_{t'-1}^d, P_{t'-1}} P(T_t | N_{t'}^d, M_t, M_{t'}, N_{t'-1}^d, P_{t'-1}) P(M_{t'}, N_{t'-1}^d, P_{t'-1}).$$

To infer the causal impact of droplet number density on cloud type, the causal network shown in Figure 6 was developed from our understanding of the underlying processes of the

aerosol–cloud interactions. The network allows for the causal effect of droplet number density (used as a proxy for aerosol concentration) on cloud type to be estimated from observational satellite images based on the backdoor adjustment^[15]. That is, the influence of the observed and unobserved confounders– the in-cloud circulations – are removed using the process of marginalization shown in Theorem 1. The marginalization process requires past observations of initial droplet number density and precipitation, and concurrent measurements of meteorology. Importantly, this means that predictions can still be made at night time when measurements of droplet number density and precipitation from satellite observations are no longer available.

The causal inference model was then developed using a Recurrent Neural Network (RNN) trained on the dataset of over 20,000 time-series of cloud structures. The model relies on several assumptions, including that the aerosol intervention is present at the beginning of the time series, however it is believed that these assumptions are generally true.

EVALUATION CRITERIA

With unsupervised and self-supervised methods, the design of evaluation criteria is of critical importance. Hypothesizing that observed cloud types will reflect fundamentally different distributions of cloud properties, we retain derived cloud properties (e.g. cloud liquid water path, cloud optical thickness, cloud droplet effective radius) for our evaluation criteria and only train on the raw SEVIRI channels. We observe the distribution of these properties under each cloud type. The more characteristic and defined the distribution is, the better is our cloud type embedding. These properties are heuristically derived from retrieval data and reflect an injection of domain knowledge and scientific study unbiased by our machine learning experiment.

We relied on the domain knowledge of our expert mentors and teammates to assess some design parameters which fell beyond the scope of the type property distributions. Our experts chose the number of cloud types (used for the mixture-of-experts and InfoGAN models) and the number of previous time-steps to use in our self-supervised mixture-of-experts implementation.

Confounding our evaluation criteria was the problem that cloud retrieval properties were only available during the day. The cloud property retrieval methods^[17] only perform reliably with the inclusion of visible spectra bands, which capture light reflected by the sun. This meant that evaluation data were only valid between approximately 09:00 and 16:00 for every day in our data, biasing the evaluation of our results.

For the causal model, we evaluate interventions on the cloud droplet number and visualise the resulting cloud types. We compare these with observed cloud types and assess our causal model using expert judgement.

RESULTS

We present results for our three cloud type models and our causal analysis.

Unsupervised Methods

We show results for our tile-to-vec and InfoGAN unsupervised methods in Figures 7 and 8 respectively. Tile-to-vec representations, visualised using the visible spectra, show how the user can specify a number of clusters into which to categorize latent space representations. The strength of this method is shown, with clear clusters emerging for different cloud meso-structures. There are, however, also clusters which do not clearly show meso-structures, such as Cluster 4 and 7 in Figure 7, which appear to reflect the availability of visible light, non-cumulus clouds, are patches over land area, or other interference.

The samples corresponding to different InfoGAN conditions are shown in Figure 8. The InfoGAN classifications better capture the variety of cloud meso-structures observed in the visible spectra representations, better capturing clear sky and closed cells, a variety of open cell structures, and also patches over land.

Figure 7: Tile-to-Vec Cluster Representations

Figure 8: InfoGAN Conditioning Representations

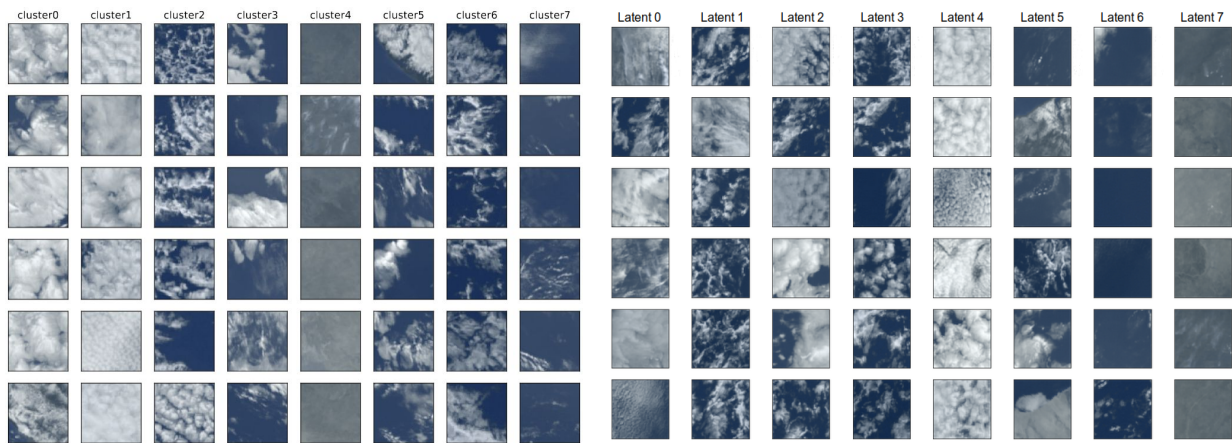
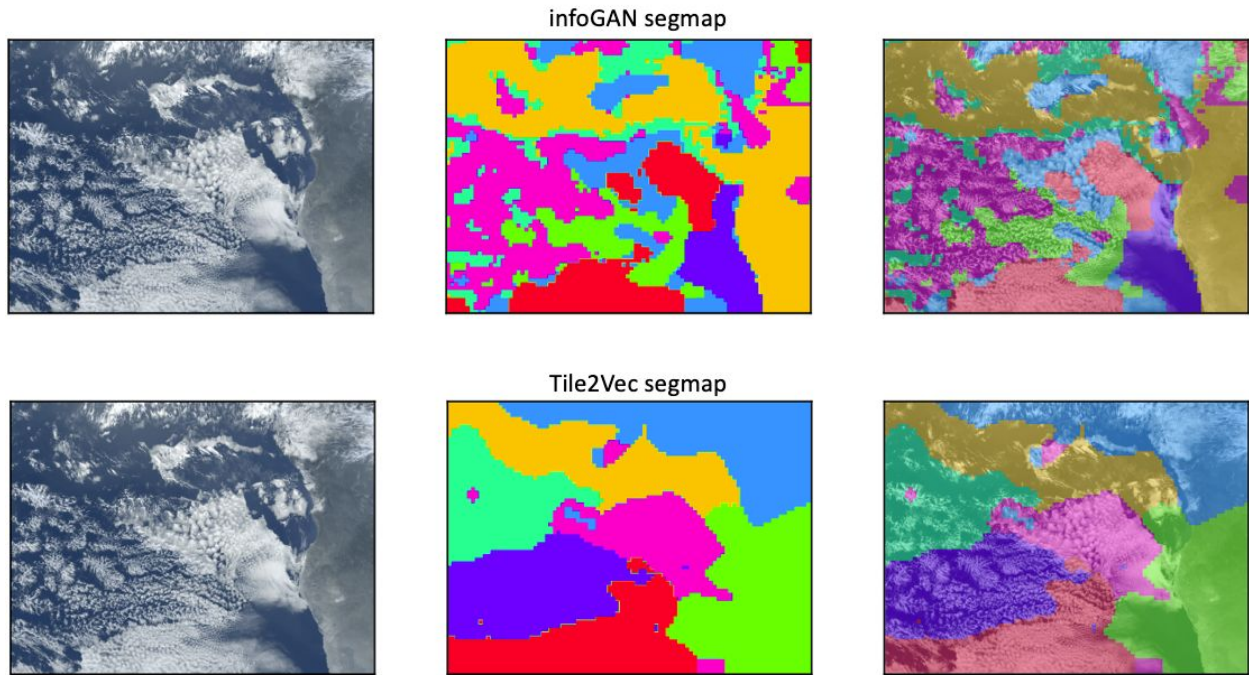


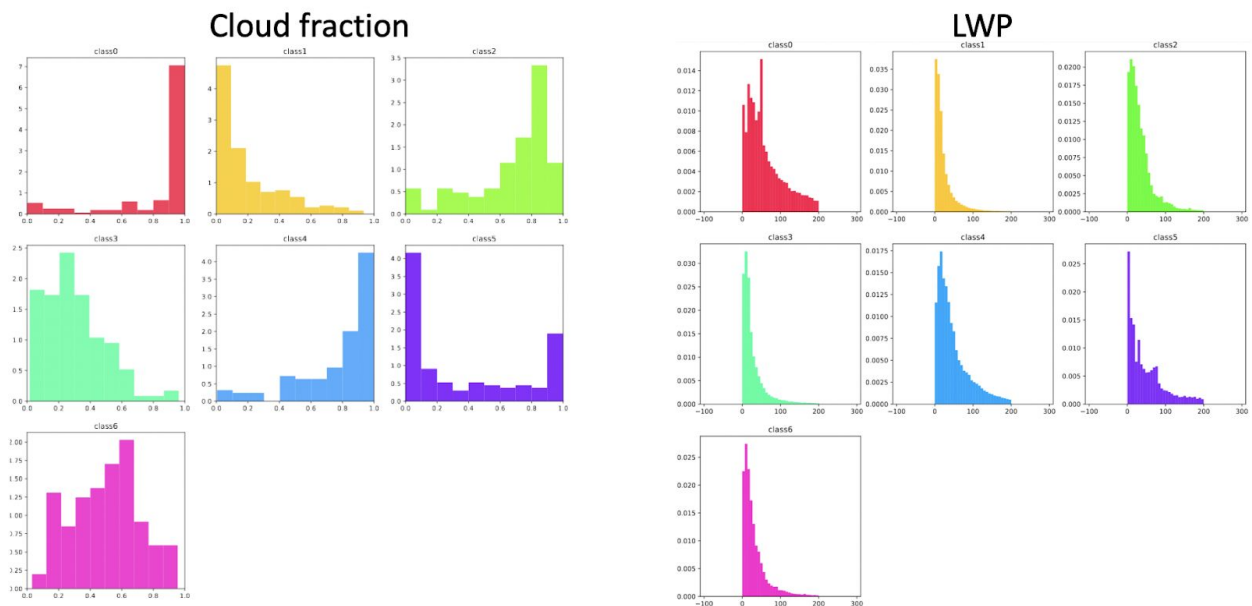
Figure 9 shows segmentation maps for both InfoGAN and Tile2Vec implementations, with colors representing different classes. With few exceptions, the Tile2Vec model classes are spatially clustered, indicating the anchor-neighbour-distant algorithm used to train the Tile2Vec model has embedded geographic bias in the cloud types. The increased detail captured by the InfoGAN model shows the transition between closed and open cell classes, and offers more differentiation between cloud types.

Figure 9: InfoGAN and Tile2VEC Segmentation Map Comparison



An evaluation of the InfoGAN model is shown in Figure 10. We show that the distributions of cloud fraction under each cloud type are distinct and indicate an effective classification. The distributions of liquid water path are not as defined.

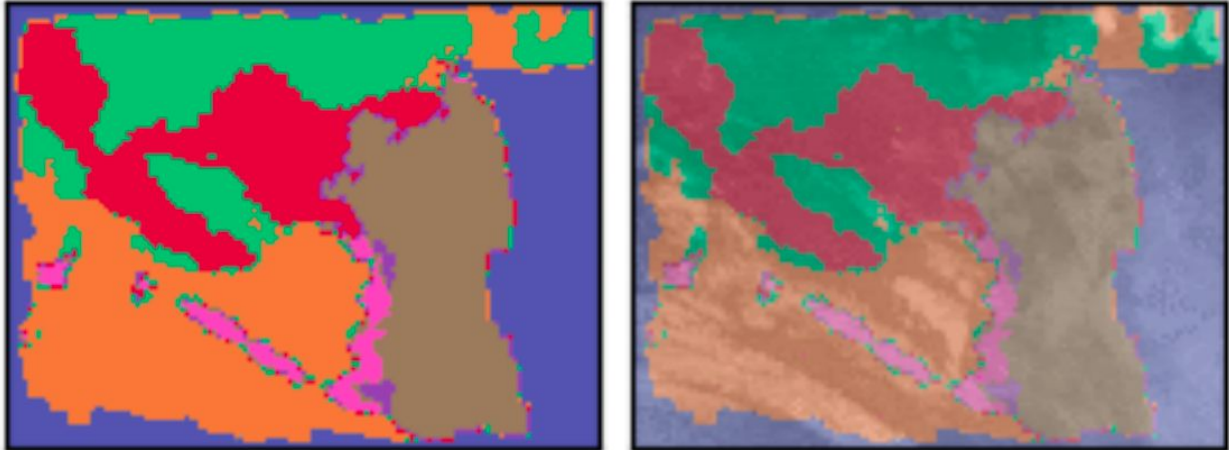
Figure 10: Cloud property distributions for InfoGAN evaluation



Mixture of Experts Implementation

We produce segmentation maps for the mixture-of-experts model by running forward inference on a sample of trajectories, see Figure 11. The mixture-of-experts model also identifies clouds in transition between type.

Figure 11: Mixture-of-experts segmentation map



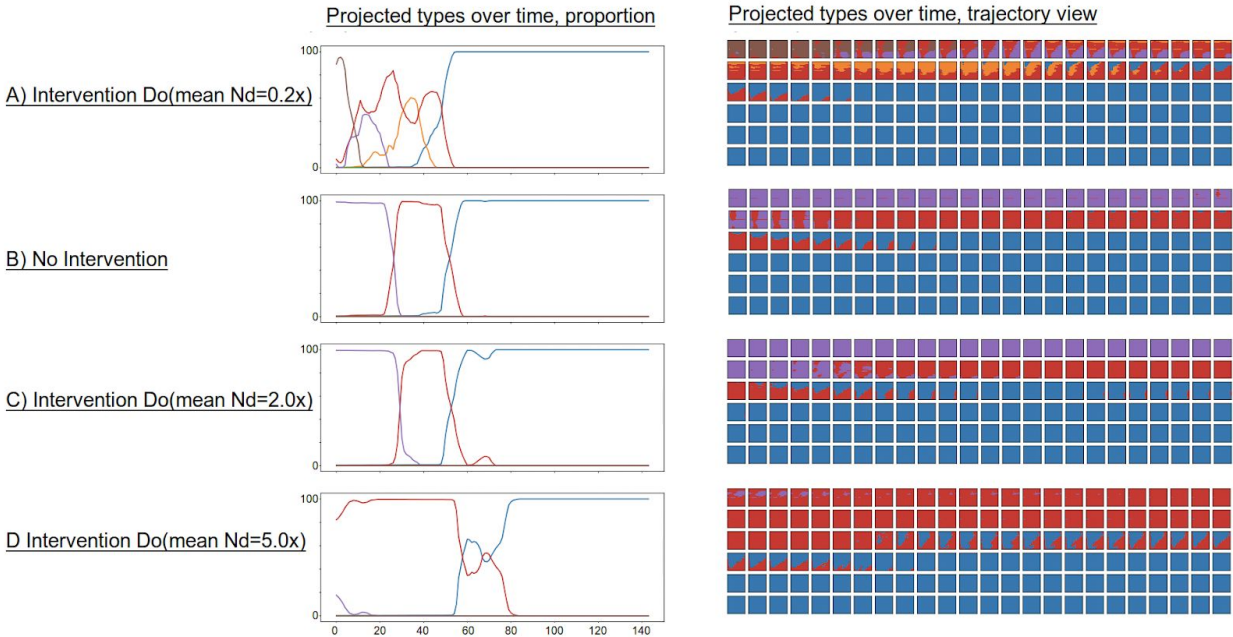
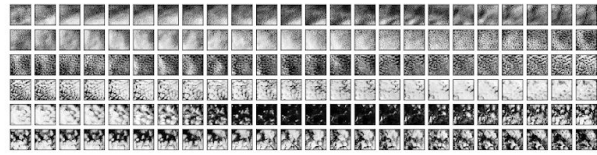
Causal Analysis

Predictions of cloud structure occurrence using the causal model are shown in Figure 12. The model ingest a time-series of real cloud observations, and predicts how the observed cloud types would change for a given droplet number density intervention for a single trajectory.

The figure illustrates the predictions of cloud type frequency for interventions of: A; $\sim 0.2x$, B; $1x$ (no intervention), C; $\sim 2x$ and D; $\sim 5x$ on cloud droplet number. The different color lines represent the different cloud type classifications including clear sky, broken cumulus, stratus, and various types of stratocumulus cloud.

Figure 12: Cloud types from causal intervention on droplet number

Single trajectory CH9 (IR10.8)
Retrievals



For the no-intervention case, we observe a mixture of closed-cell stratocumulus and cumulus clouds prior to clear sky. In the reduced droplet number density situation we see a large increase in the proportion of broken cumulus. Contrary to this, for the increased droplet number density cases we see an increase in the proportion of closed-cell stratocumulus and a delay in the length of time taken for clear sky conditions.

These predictions therefore support that an increase in aerosol concentration and hence droplet number density leads to an increase in the occurrence of close-cell stratocumulus, and an increase of cloud lifetime.

IMPLEMENTATION AND REPRODUCIBILITY

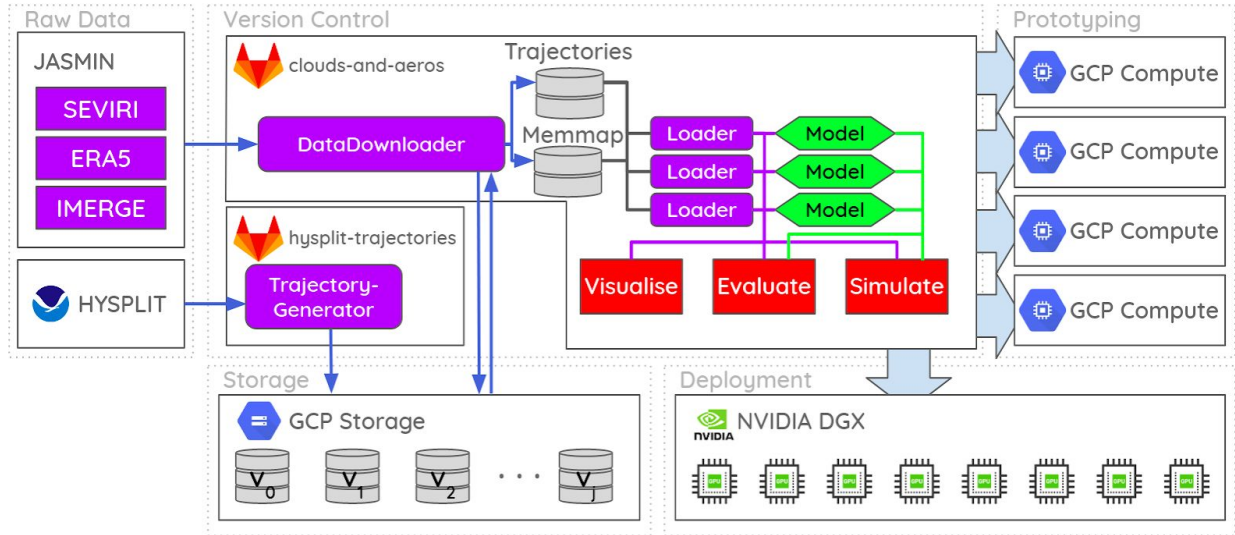
We implement our machine learning utilities, pipeline, and analysis in two shared code repositories: the first for producing trajectory data² and the second for the machine learning implementation.³ Our implementation is represented in Figure 13. The two repositories have substantially different dependencies and so are prepared separately. The preparation of trajectories required approximately 1tb of meteorological data to be mirrored locally which were not otherwise required in the machine learning pipeline. Additionally, the HYSPLIT module is

² <https://gitlab.com/frontierdevelopmentlab/fdl-europe-2020-clouds-and-aerosols/hysplit-trajectories>

³ <https://gitlab.com/frontierdevelopmentlab/fdl-europe-2020-clouds-and-aerosols/clouds-and-aeros>

incompatible with primary Ubuntu distributions, and needed to be implemented on a RedHat virtual machine. Trajectories prepared by the HYSPLIT codebase are mirrored to Google Cloud Storage and are retrieved by the machine learning pipeline. For reproduction, we recommend obtaining the trajectories already prepared.

Figure 13: Implementation conceptual drawing



Our machine learning pipeline is flexible across platforms and GPU hardware availability. Local permanent disks were provisioned to mirror data from cloud storage. Due to our unique lagrangian sampling method, our 350gb training data was written to numpy memory-mapped arrays, allowing us to rapidly sample slices by lazily loading slices into memory. During training, we prototyped and implemented on multiple GCP AI Notebook Instances as well a dedicated DGX DeepLearning workstation provided by NVidia-Scan. Machine learning models were implemented in PyTorch, experiment monitoring was provided by TensorBoard, and record-keeping was implemented with Sacred. Reproducibility instructions are available in both repositories.

FUTURE WORK

The combination of novel cloud classification techniques and causal inference of time series of classified satellite observations has shown great potential for investigating the complex aerosol impacts on cloud structure and lifetime. However, as these techniques are new and experimental, further evaluation is required to ensure that the results provide solid evidence for real cloud processes. Several methods have been developed for the evaluation of the cloud classification method, including investigating the cloud properties of each cloud type – including cloud fraction and liquid water path – to ensure that each cloud type is both consistent and differentiable from others. Further methods to investigate the structures within each cloud type, including Fourier analysis, have also been investigated.

The causal inference model also requires evaluation, both of the model itself and of the assumptions that have been made to construct the causal network. Although we believe these assumptions to hold true – particularly that of the aerosol influence being present at the beginning of the time series – these need verification for the results to be trusted. Furthermore, the predicted time-series for different droplet number concentrations need to be compared with real time series in order to evaluate the accuracy of the model.

Finally, although we are able to predict the relative occurrence and lifetime of different cloud types with our model, we are not able to predict how these changes would affect the climate. Further work will involve predicting the radiative forcing impacts of cloud structure changes in order to better understand the climate impacts of aerosol effects on cloud structure and lifetime.

CONCLUSION

In this work, we have used machine learning to investigate the causal nature of aerosol-cloud interactions. We first determined cloud types using a variety of unsupervised and self-supervised methods, and then trained a causal model using a sequence model. We provide early evidence to show that the presence of aerosols, proxied by an increased cloud droplet concentration, leads to longer lifetimes of closed-cell meso-scale structures. Significant, but promising, work remains to verify the robustness of our findings and what they mean for the future of the climate.

REFERENCES

- [1] Mueller, Richard, et al. "The role of the effective cloud albedo for climate monitoring and analysis." *Remote Sensing* 3.11 (2011): 2305-2320.
- [2] Zhou, Xiaoli, Pavlos Kollias, and Ernie R. Lewis. "Clouds, precipitation, and marine boundary layer structure during the MAGIC field campaign." *Journal of Climate* 28.6 (2015): 2420-2442.
- [3] Rossow, William B., Carl Delo, and Brian Cairns. "Implications of the observed mesoscale variations of clouds for the Earth's radiation budget." *Journal of climate* 15.6 (2002): 557-585.
- [4] McCoy, Isabel L., Robert Wood, and Jennifer K. Fletcher. "Identifying meteorological controls on open and closed mesoscale cellular convection associated with marine cold air outbreaks." *Journal of Geophysical Research: Atmospheres* 122.21 (2017): 11-678.
- [5] Wood, R. (2012). Stratocumulous clouds. *Monthly Weather Review*, 140: 2373--, DOI: 10.1175/MWR-D-11-00121.1
- [6] Bellouin, N. "Role in Climate Change." *Encyclopedia of Atmospheric Sciences* 1 (2014): 76.
- [7] McCoy, D. T., Field, P. R., Schmidt, A., Grosvenor, D. P., Bender, F. A.-M., Shipway, B. J., Hill, A. A., Wilkinson, J. M., and Elsaesser, G. S.: Aerosol midlatitude cyclone indirect effects in observations and high-resolution simulations, *Atmos. Chem. Phys.*, 18, 5821–5846, <https://doi.org/10.5194/acp-18-5821-2018>, 2018.
- [8] Christensen, Matthew W., William K. Jones, and Philip Stier. "Aerosols enhance cloud lifetime and brightness along the stratus-to-cumulus transition." *Proceedings of the National Academy of Sciences* 117.30 (2020): 17591-17598.
- [9] Ghate, V. P., Albrecht, B. A., Kollias, P., Jonsson, H. H. & Breed, D. W. Cloud seeding as a technique for studying aerosol-cloud interactions in marine stratocumulus. *Geophys. Res. Lett.* 34, 5 (2007)
- [10] Lawrence, Mark G., et al. "Evaluating climate geoengineering proposals in the context of the Paris Agreement temperature goals." *Nature communications* 9.1 (2018): 1-19.
- [11] AR5
- [12] Stevens, Bjorn, et al. "Sugar, gravel, fish and flowers: Mesoscale cloud patterns in the trade winds." *Quarterly Journal of the Royal Meteorological Society* 146.726 (2020): 141-152.
- [13] Wood, Robert, and Dennis L. Hartmann. "Spatial variability of liquid water path in marine low cloud: The importance of mesoscale cellular convection." *Journal of Climate* 19.9 (2006): 1748-1764.
- [14] Denby, L. "Discovering the importance of mesoscale cloud organization through unsupervised classification." *Geophysical Research Letters* 47.1 (2020): e2019GL085190.
- [15] Pearl, Judea. "Causality: Models, Reasoning, and Inference." (2000).
- [16] Schmid, J. "The SEVIRI instrument." *Proceedings of the 2000 EUMETSAT meteorological satellite data user's conference, Bologna, Italy*. Vol. 29. 2000.
- [17] Platnick, Steven, et al. "The MODIS cloud products: Algorithms and examples from Terra." *IEEE Transactions on Geoscience and Remote Sensing* 41.2 (2003): 459-473.
- [18] Hersbach, Hans, et al. "The ERA5 global reanalysis." *Quarterly Journal of the Royal Meteorological Society* 146.730 (2020): 1999-2049.
- [19] Hou, A. Y., and et al, 2014: The Global Precipitation Measurement mission. *Bull. Amer. Meteor. Soc.*, 95, 701–722, <https://doi.org/10.1175/BAMS-D-13-00164.1>.

- [20] Stephens, Graeme L., et al. "The CloudSat mission and the A-Train: A new dimension of space-based observations of clouds and precipitation." *Bulletin of the American Meteorological Society* 83.12 (2002): 1771-1790.
- [21] Jean, Neal, et al. "Tile2vec: Unsupervised representation learning for spatially distributed data." *Proceedings of the AAAI Conference on Artificial Intelligence*. Vol. 33. 2019.
- [22] Chen, Xi, et al. "Infogan: Interpretable representation learning by information maximizing generative adversarial nets." *Advances in neural information processing systems*. 2016.
- [23] Yuan, Tianle. "Understanding low cloud mesoscale morphology with an information maximizing generative adversarial network." (2019).
- [24] Christensen, Matthew W., William K. Jones, and Philip Stier. "Aerosols enhance cloud lifetime and brightness along the stratus-to-cumulus transition." *Proceedings of the National Academy of Sciences* 117.30 (2020): 17591-17598.
- [25] Draxler, R. R., and G. D. Rolph. "HYSPLIT (HYbrid Single-Particle Lagrangian Integrated Trajectory) model access via NOAA ARL READY website (<http://ready.arl.noaa.gov/HYSPLIT.php>). NOAA Air Resources Laboratory." *Silver Spring, MD* 25 (2010).
- [26] Zhang, Dejiao, et al. "Deep unsupervised clustering using mixture of autoencoders." *arXiv preprint arXiv:1712.07788* (2017).